PHYSICAL REVIEW E **84**, 015302(R) (2011)

Universality and scaling behavior of injected power in elastic turbulence in wormlike micellar gel

Sayantan Majumdar and A. K. Sood*
Department of Physics, Indian Institute of Science, Bangalore 560 012, India
(Received 22 March 2011; revised manuscript received 17 June 2011; published 20 July 2011)

We study the statistical properties of spatially averaged global injected power fluctuations for Taylor-Couette flow of a wormlike micellar gel formed by surfactant cetyltrimethylammonium tosylate. At sufficiently high Weissenberg numbers the shear rate, and hence the injected power $p(t)$, at a constant applied stress shows large irregular fluctuations in time. The nature of the probability distribution function (PDF) of $p(t)$ and the power-law decay of its power spectrum are very similar to that observed in recent studies of elastic turbulence for polymer solutions. Remarkably, these non-Gaussian PDFs can be well described by a universal, large deviation functional form given by the generalized Gumbel distribution observed in the context of spatially averaged global measures in diverse classes of highly correlated systems. We show by *in situ* rheology and polarized light scattering experiments that in the elastic turbulent regime the flow is spatially smooth but random in time, in agreement with a recent hypothesis for elastic turbulence.

DOI: 10.1103/PhysRevE.84.015302 PACS number(s): 47.50.−d, 83.80.Qr

Hydrodynamic instability such as turbulence is an inertia-driven phenomenon occurring at high Reynolds numbers (Re). However, for viscoelastic fluids of long polymers, similar instabilities have been observed even at a very low Re because of elastic hoop stresses generated by the stretching of the polymers in the curvilinear flow field, indicated by a high Weissenberg number (Wi) [1]. The Weissenberg number, defined by the ratio of the time scale set by the relaxation time τ_R of the fluid to that set by the strain rate $\dot{\gamma}$, $\mathrm{Wi} = \tau_R\,\dot{\gamma} = N_1/\sigma$, with N_1 the first normal stress difference at a shear stress σ, plays the same role for elastic turbulence that Re plays in the case of inertial turbulence. The elastic turbulence [1] is a flow instability that occurs at practically zero Re ($\mathrm{Re} \ll 1$) and high Wi ($\mathrm{Wi} \gg 1$).

In past few years the statistics and scaling properties of the injected power fluctuations have been studied in detail both experimentally and numerically for inertial turbulence [2–7] in von Kármán swirling flows. It has been shown that the probability distribution function (PDF) of spatially averaged global injected power shows deviation from the Gaussian nature: skewness on the side of the smaller value of the injected power. Inertial turbulence also shows spatially smooth but random in time flow behavior like elastic turbulence, below the Kolmogorov dissipation scale. Recently, similar results have emerged for power fluctuations in polymers in the context of elastic turbulence in von Kármán flow [8]. Although the sign of the asymmetry of the power fluctuations appears to be the same for both the inertial and the elastic turbulence, the magnitude of the normalized third moment or skewness varies in different studies. For some cases, such as in Ref. [6], the PDFs are very skewed, ~ -1, but in many other cases [7,8] this value is ~ -0.2. It has been argued that averaging over many independent large-scale structures decreases the skewness of the global quantities. Very recently, the flow behavior of wormlike micellar systems has been shown to have signatures of elastic turbulence [9].In this paper we study the statistics and universality properties of spatially averaged global injected power in the case of unstable flow at high Wi and very low Re for wormlike micellar gels. These studies are important for wormlike micellar systems since wormlike micelles have additional relaxation mechanisms due to scission-reattachment dynamics compared to polymers [10]. This motivated us to study the spatially averaged global injected power fluctuations for Taylor-Couette flow of a shear-thinning wormlike micellar solution that shows elastic turbulence. At sufficiently high Wi, the time series of injected power $p(t) = \sigma\ \dot{\gamma}\ (t) V_s$ [where σ is the applied stress, $\dot{\gamma}\ (t)$ is the resulting shear rate, and V_s is the volume of the sample] at a fixed shear stress shows large irregular fluctuations. The PDFs of $p(t)$ deviate from the Gaussian nature with skewness toward the low-power side with respect to $\langle p(t) \rangle$ and the values of skewness obtained are similar to that in Newtonian fluids [7] and polymer flows [8] despite the differences in the flow profiles in von Kármán and Taylor-Couette geometries. Moreover, the three systems discussed above, namely, a Newtonian fluid [7], polymer solutions [8], and the present wormlike micellar gel, follow different routes to turbulence from the laminar flow because of their completely different dynamics and relaxation mechanisms that make their statistical similarities in the turbulent regime even more nontrivial. We show that the non-Gaussian PDF of the injected power $p(t)$ for elastic turbulence in wormlike micellar systems can be described by a universal, large deviation functional form given by the generalized Gumbel (GG) distribution, observed for fluctuations of injected power in inertial turbulent flows [6,11,12] and many other correlated systems [13–21]. Physically, when the correlation length becomes comparable to the system size, the system cannot be divided into a large number of independent domains for any global or spatially averaged measurements; hence the central limit theorem no longer holds and deviations from the Gaussian statistics are observed. To see this correlation directly, we performed *in situ* polarized light scattering and rheology experiments as described in detail in Ref. [22]. In the turbulent regime, the scattered light signals obtained from the gap of the transparent Couette cell show random fluctuations. A calculation of spatial and temporal correlation functions of the scattered intensity

*asood@physics.iisc.ernet.in

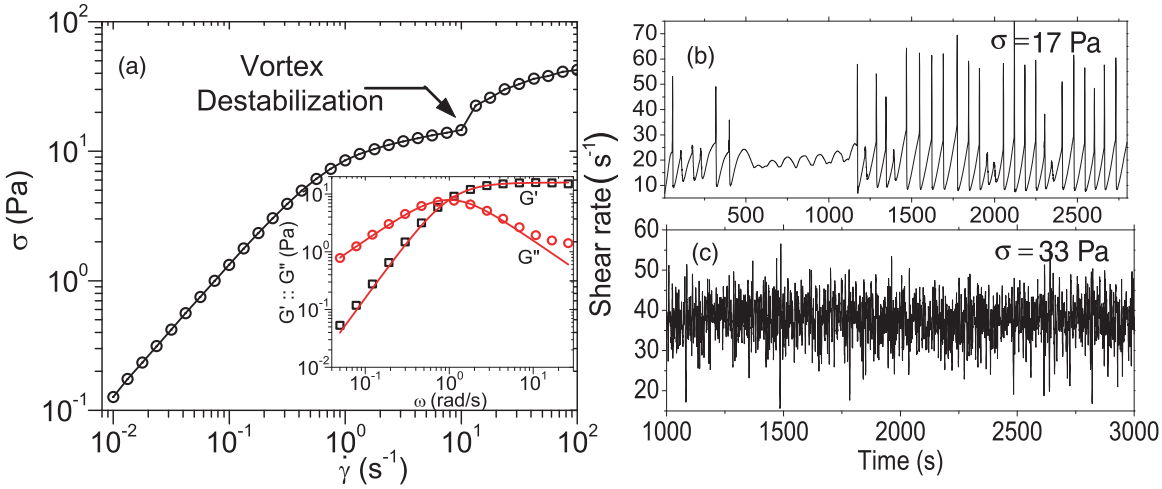

FIG. 1. (Color online) (a) Shear stress σ as a function of shear rate $\dot{\gamma}$ for CTAT 2 wt. % + 100 mM NaCl. The inset shows the storage G' and loss G'' moduli as functions of angular frequency ω. Solid lines indicate the fit to the single-relaxation Maxwell model. Also shown is the shear rate as a function of time for different applied shear stresses: (b) $\sigma = 17$ Pa and (c) $\sigma = 33$ Pa.

fluctuations reveals that even though the time correlation is very short ranged, the system has a very-long-ranged spatial correlation, practically limited by the size of the Couette cell itself. By this direct method we show the nontrivial space-time flow behavior satisfying the criterion for elastic turbulence in micellar systems. To test the statistical robustness of the results, we repeated all the measurements in another Couette geometry with completely different aspect ratios. Both sets of results are in very good agreement with each other.

We used cetyltrimethylammonium tosylate (CTAT) 2 wt. % + 100mM NaCl in water, which forms a wormlike micellar gel for our experiments. The preparation of the sample is discussed in detail in Ref. [23]. All the experiments were carried out on a MCR300 stress-controlled rheometer (Anton PAAR, Germany) at a temperature of 26 °C. For imaging experiments, we used homemade transparent Couette geometry having an inner cylinder diameter of 23 mm, a height of 40 mm, and a gap of 1 mm (Couette A). The outer cylinder is made of transparent glass and is partially enclosed by a water circulation chamber to control the temperature (the exposed portions of the glass cell were used for imaging). A thin sheet of polarized laser beam, which was formed by placing a cylindrical lens and polarizer arrangement in front of a randomly polarized He-Ne laser (10 mW), was sent along the vorticity ($\nabla \times \mathbf{v}$) direction to illuminate the entire gap in the ($\nabla \times \mathbf{v}, \nabla v$) plane and imaging was done perpendicularly to the illuminated plane with a wide angle lens and a charge coupled device (CCD) camera (Lumenera 0.75C, 640 × 480 pixels). With this arrangement the polarization of the incident laser beam can be tuned continuously in the ($\mathbf{v}, \nabla v$) plane. All the optical components were mounted on XYZ stages for precision control. To achieve statistical accuracy, we analyze the shear-rate or shear-stress time series with almost 50 000 data points (data points from the startup transients were ignored) sampled at a frequency of 5 Hz. The experimental tolerance in the value of applied shear stress is $\sim 10^{-3}$% and for applied shear rate (obtained through a feedback mechanism in our stress-controlled instrument) it is ∼1%.

The flow curve for CTAT 2 wt. % + 100mM NaCl is shown in Fig. 1(a). The system shows Maxwellian behavior [10] with a single-relaxation time $\tau_R \sim 1$ s [Fig. 1(a) inset]. In the nonlinear regime, *in situ* imaging experiments do not show shear banding, but reveal Taylor vortex flow from the onset of the shear-thinning plateau. Also, at $\dot{\gamma} \sim 10$, there is a sudden jump in the stress value, indicating the enhanced flow resistance because of the onset of elastic turbulence. Beyond this value of $\dot{\gamma}$ the Taylor vortices get destabilized and move randomly, manifesting in large fluctuations in shear rate at a constant applied shear stress and vice versa [22,24]. We study the temporal dynamics of the system in the nonlinear regime for applied shear-stress values of 17 and 33 Pa. The shear rate does not exhibit fluctuations at stress values less than 17 Pa. For a stress value of 17 Pa, which corresponds to the onset of elastic turbulence, the shear rate shows intermittent behavior, indicating that the system becomes unstable and shows huge fluctuations, as shown in Fig. 1(b). Figure 1(c) indicates that the shear rate fluctuates randomly with time for a stress value of 33 Pa. This is the elastic turbulence regime and all further statistical analysis herein is done in this regime. The dynamics of shear rate exactly correlates with the dynamics of the Taylor vortices, as observed in Ref. [22].

The PDFs $\Pi(p)$ and $\Pi(y)$ of injected power p in the turbulent regime for applied shear-stress values σ = 34–36 Pa are shown in Fig. 2(a), where we see that with increasing σ, the peak of the corresponding PDF shifts toward a higher value of the injected power. In Fig. 2(b) the same PDFs are plotted in terms of a reduced value of the injected power $y = \frac{\Delta P}{\Gamma}$, where $\Delta P = p(t) - \langle p(t) \rangle$. Here $\langle p(t) \rangle$ and Γ are, respectively, the mean and the standard deviation of $p(t)$. It can be seen that all the curves collapse into a master curve that deviates from the Gaussian function with negative skewness. The dotted line is a fit to the Gaussian function to show the non-Gaussian nature of the master PDF. We now show that the non-Gaussian PDF of the injected power $p(t)$ shown in Fig. 2(b) is well represented by GG distribution given by [25,26]

$$\Pi(y) = K(a) e^{a\{-b(a)[y+z(a)]-e^{-b[y+z(a)]}\}}. \quad (1)$$

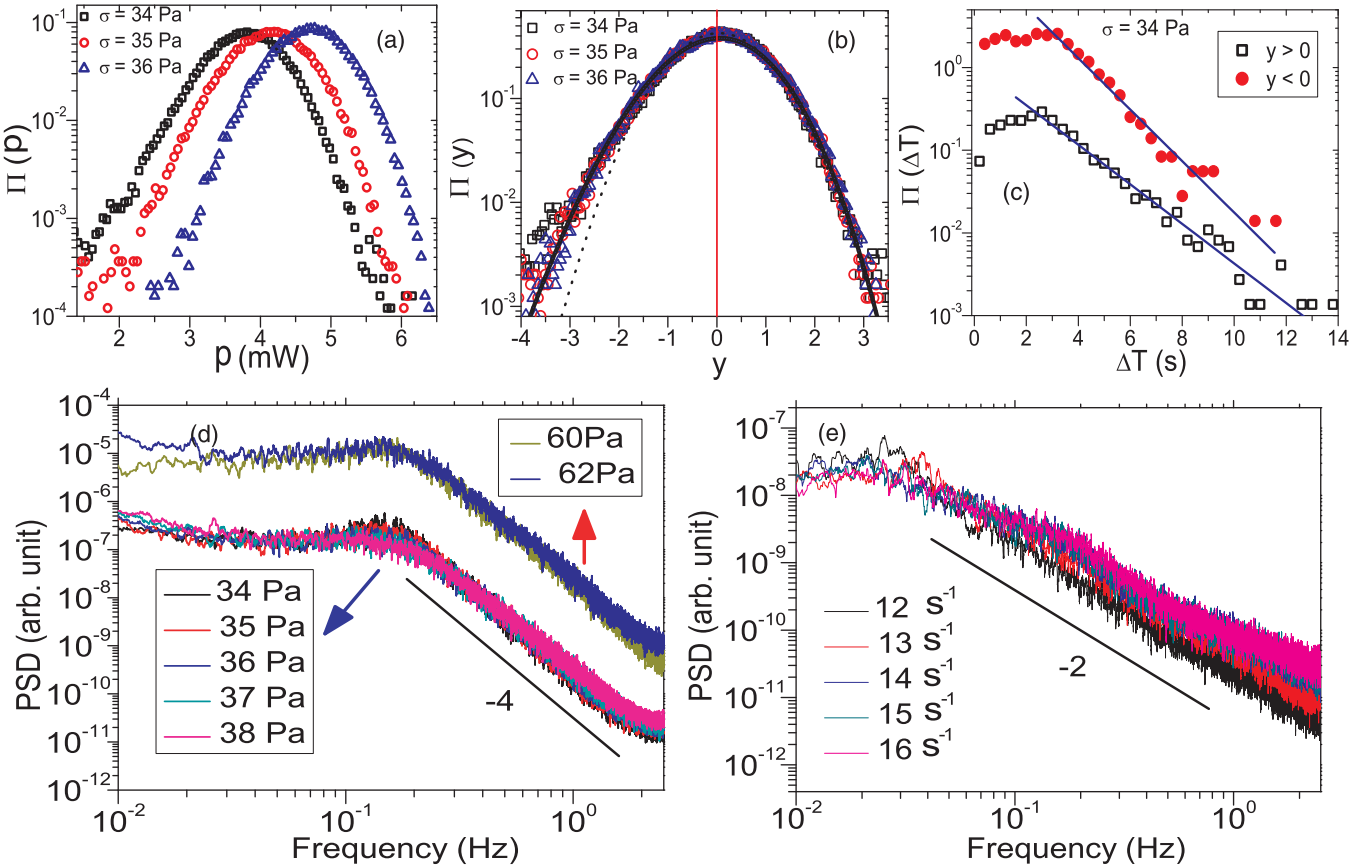

FIG. 2. (Color online) PDFs $\Pi(p)$ and $\Pi(y)$ of injected power for different applied stress values in the elastic turbulent regime: $\sigma = 34$, 35, and 36 in terms of (a) raw and (b) reduced (defined in the text) injected power. The solid line in (b) indicates the simulated curve using the GG distribution for $a = 39$ and the dotted line is the fit to the Gaussian function. (c) PDF $\Pi(y)$ of spike width for $y > 0$ (open squares) and $y < 0$ (solid circles) for an applied stress σ of 34 Pa. The solid lines indicate the exponential fits $\Pi(\Delta T) = \Pi_0 e^{-\Delta T/\tau}$ to the data. For clarity the PDFs for $y < 0$ have been shifted by a multiplicative factor of 10. (d) PSD of injected power fluctuations for applied stress values of 32–36 Pa (for Couette A) and also for 60 and 62 Pa (for Couette B, described in the text). The straight solid line indicates a power-law exponent of −4. The curves for Couette B are shifted by a multiplicative factor of 100 for clarity. (e) PSD of injected power in constant shear-rate mode for 12–16 s^{-1} (Couette A). The straight solid line indicates a power-law exponent of −2.

Equation (1) has a single parameter a that is again fixed by the skewness of the distribution as $\langle y^3 \rangle = 1/\sqrt{a}$. All other parameters are related to a as follows: $b(a)^2 = d^2 \ln\Gamma(a)/da^2$, $z(a) = \frac{1}{b}[\ln a - d\ln\Gamma(a)/da]$, and $K(a) = ba^a/\Gamma(a)$, where $\Gamma(a)$ is the Gamma function. The non-Gaussian PDF with negative skewness matches perfectly to the simulated curve given by the GG distribution [Eq. (1)], as shown by the solid lines in Fig. 2(b), over approximately three orders of magnitude with the value of the parameter $a = 39$ estimated from the third moment of the experimentally measured reduced injected power $\langle y^3 \rangle$. Figure 2(c) shows the distribution of temporal spike width ΔT (persistence time of a single fluctuation event) for the reduced injected power y above and below its mean value ($\langle y \rangle = 0$) for an applied stress of 34 Pa. For both the cases $\Pi(\Delta T)$ shows exponential tails over two orders of magnitude, as shown by the linear fits on a log-linear scale, indicating the statistical independence of the large time events, although for short times they remain strongly correlated. The time constants for the exponential decays are $\tau = 2.2$ s for $y > 0$ and 1.4 s for $y < 0$. The mean spike width $\langle \Delta T \rangle = 2.8$ s for $y > 0$ and 2.6 s for $y < 0$. Since the skewness of $\Pi(y) < 0$ [Fig. 2(b)], the higher values of $\langle \Delta T \rangle$ and τ for $y > 0$ compared to those for $y < 0$ imply that the large intermittent negative fluctuations have shorter lifetimes. The skewness of the distribution on the negative side has also been seen in polymer solutions [27], which has been postulated to be due to accumulation of the elastic stress near the static boundary. This observation is counterintuitive to the finding that the shear rate is higher near the inner cylinder and hence would result in larger stresses near the inner cylinder. More work is needed to clarify our results.

The power spectral density (PSD) of $p(t)$, i.e., $\dot{\gamma}(t)$, at different applied stress values in the turbulent regime are shown in Fig. 2(d), which displays a power-law decay with an exponent $\beta = -4$ over five orders of magnitude and a smeared peak at ∼0.15 Hz. This value of β satisfies the criterion ($|\beta| > 3$) derived by Fouxon and Lebedev [28] for the elastic turbulence. To see the statistical robustness of the exponent β, we repeated all the experiments in another Couette geometry having a different aspect ratio: an inner cylinder diameter of 32 mm, a height of 16.5 mm, and a gap of 2 mm (Couette B). Here the onset of elastic turbulence occurs at a much higher value of applied stress (∼50 Pa). The difference in the onset of elastic turbulence can come from the difference

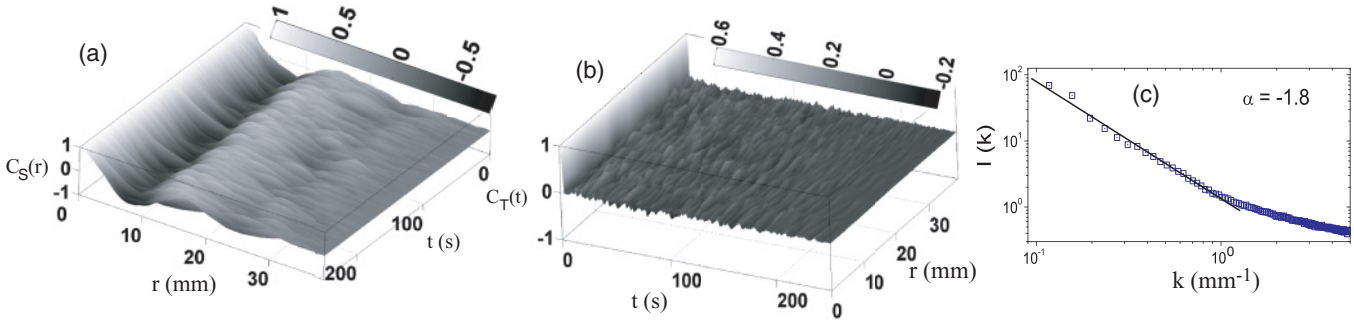

FIG. 3. (Color online) Space-time behavior of (a) normalized spatial correlation function $C_S(r)$ and (b) normalized temporal correlation function $C_T(t)$. (c) Time-averaged spatial Fourier amplitude $I(k)$ of scattered intensity as a function of wave vector k (=1/l); the solid line is a power-law fit with exponent −1.8 to the data. The applied stress $\sigma = 33$ Pa in all cases.

in curvatures of the two geometries. The value of β obtained for the PSD evaluated at the applied stress values of 60 and 62 Pa is again −4, as shown in Fig. 2(d). The PSD of $p(t)$, i.e., $\sigma(t)$, at a constant shear rate for Couette A is shown in Fig. 2(e), where again a power law with a slope of −2 is observed that does not satisfy the Fouxon-Lebedev criterion. We do not understand the origin of the different power laws seen in controlled-shear-stress and controlled-shear-rate experiments.

To look for any long-range correlations in the system in the turbulent regime we performed *in situ* polarized light scattering studies as described in detail in Ref. [22]. We image the gap of the Couette cell A as a function of time in the $(\nabla \times \mathbf{v}, \nabla v)$ plane in the turbulent regime with a CCD camera at a frame rate of 1 Hz. This frame rate is sufficient to capture the correlated dynamics in the system since the injected power $p(t)$ has a correlation time of ∼3 s. The image of the entire gap (∼40 × 1 mm) is represented by a slice of 370 × 11 pixels and we analyze 250 such slices in the turbulent regime. We study the space-time distribution of scattered intensity $I(r,t)$ by studying the intensity along a vertical cut that covers the entire length of the cell along the vorticity direction (370 × 1 pixels) chosen near the center of the gap of the Couette cell and then stacking them at different times as the space-time plot (STP). The STP of the scattered intensity distribution in the turbulent regime is quite random (data not shown). The normalized spatial correlation functions $C_S(r) = \langle I(r')I(r + r')\rangle_{r'}$ evaluated at different times in the turbulent regime are shown in Fig. 3(a), which clearly reveals that the scattered intensity is correlated spatially over the entire length of the Couette geometry and practically limited by the size of the container at every t. Similarly, we also calculate the normalized temporal correlation function $C_T(t) = \langle I(t')I(t + t')\rangle_{t'}$ for all the pixels along the cut. The correlation function $C_T(t)$ is extremely short lived, almost δ correlated (up to our time resolution), as shown in Fig. 3(b). The temporal correlation function monotonically goes to the base line over ∼1 s, as has been confirmed by a higher image grabbing rate of 3 Hz (not shown). These observations clearly indicate that even though the spatially averaged injected power fluctuates randomly in time, the spatial structures remain intact and they move randomly in time.Figure 3(c) shows the plot of a time-averaged spatial Fourier transform of scattered intensity along the vertical cut mentioned above, which shows a power-law decay $[I(k) \sim k^{\alpha}]$ with exponent $\alpha = -1.8$ (similar to that obtained in Ref. [9]) over a length scale spanning ∼ 1–10 mm.

In conclusion, we have studied the universality and scaling properties of spatially averaged global injected power $p(t)$ in the context of elastic turbulence in a shear-thinning worm-like micellar gel. The non-Gaussian probability distribution functions show a negative skewness, which is very similar to the case of polymer solutions [8]. The power spectral density of $p(t)$ shows a power-law behavior with a decay exponent $\beta = -4$ (< -3), which is a signature of elastic turbulence [28]. However, the decay exponent β is very different (∼−2) for a constant shear-rate run, which is not understood. We showed a universal scaling of the non-Gaussian PDF of $p(t)$ in terms of generalized Gumbel distribution, which is observed in many cases of spatially averaged global measures for a diverse class of highly correlated systems [13–21]. Studies of *in situ* polarized light scattering clearly show the presence of spatially long-ranged correlated dynamics in the turbulent regime, although the temporal correlations are short ranged. We believe that the presence of this long-ranged spatial correlation is responsible for the GG distribution of the spatially averaged global injected power. This kind of universality is similar to that observed for inertial turbulence [6,11,12]. The intermittent nature of the injected power below the mean value as compared to its value above the mean has been postulated to be associated with the nature of the elastic stress field in the system [27]. We believe that our work will motivate further experimental and theoretical studies on the fascinating phenomenon of elastic turbulence in soft matter.

A.K.S. thanks Council of Scientific and Industrial Research, India for financial support and S.M. thanks University Grants Commission of India for financial support.

[1] A. Groisman and V. Steinberg, Nature (London) **405**, 53 (2000); New J. Phys. **6**, 29 (2004).
[2] S. Fauve *et al.*, J. Phys. II (France) **3**, 271 (1993).
[3] P. Abry *et al.*, J. Phys. II (France) **4**, 725 (1994).
[4] O. Cadot *et al.*, Phys. Fluids **7**, 630 (1995).
[5] R. Labbe *et al.*, J. Phys. II (France) **6**, 1099 (1996).

[6] J. F. Pinton, P. C. W. Holdsworth, and R. Labbe, Phys. Rev. E **60**, 2452(R) (1999), and references cited therein.
[7] J. H. Titon and O. Cadot, Phys. Fluids **15**, 625 (2003).
[8] Y. Jun and V. Steinberg, Phys. Rev. Lett. **102**, 124503 (2009).
[9] M. A. Fardin *et al.*, Phys. Rev. Lett. **104**, 178303 (2010).
[10] M. E. Cates, Macromolecules **20**, 2289 (1987).
[11] S. T. Bramwell *et al.*, Nature (London) **396**, 552 (1998).
[12] B. Portelli, P. C. W. Holdsworth, and J. F. Pinton, Phys. Rev. Lett. **90**, 104501 (2003).
[13] S. Joubaud, A. Petrosyan, S. Ciliberto, and N. B. Garnier, Phys. Rev. Lett. **100**, 180601 (2008).
[14] W. I. Goldburg, Y. Y. Goldschmidt, and H. Kellay, Phys. Rev. Lett. **87**, 245502 (2001).
[15] T. Toth-Katona and J. T. Gleeson, Phys. Rev. Lett. **91**, 264501 (2003).
[16] T. Antal, M. Droz, G. Gyorgyi, and Z. Rácz, Phys. Rev. Lett. **87**, 240601 (2001).
[17] B. P. Van Milligen *et al.*, Phys. Plasmas **12**, 052507 (2005).
[18] C. Pennetta *et al.*, Semicond. Sci. Technol. **19**, 098001 (2005).
[19] J. J. Brey, M. I. García de Soria, P. Maynar, and M. J. Ruiz-Montero, Phys. Rev. Lett. **94**, 098001 (2005).
[20] C. Chamon and L. F. Cugliandolo, J. Stat. Mech. (2007) P07022.
[21] R. Planet, S. Santucci, and J. Ortin, Phys. Rev. Lett. **102**, 094502 (2009).
[22] R. Ganapathy, S. Majumdar, and A. K. Sood, Phys. Rev. E **78**, 021504 (2008).
[23] R. Ganapathy and A. K. Sood, Phys. Rev. Lett. **96**, 108301 (2006).
[24] R. Ganapathy, S. Majumdar, and A. K. Sood, Eur. Phys. J. B **64**, 537 (2008).
[25] S. T. Bramwell *et al.*, Phys. Rev. Lett. **84**, 3744 (2000).
[26] M. Clusel *et al.*, Europhys. Lett. **76**, 1008 (2006).
[27] T. Burghelea, E. Segre, and V. Steinberg, Phys. Rev. Lett. **96**, 214502 (2006); Phys. Fluids **19**, 053104 (2007).
[28] A. Fouxon and V. Lebedev, Phys. Fluids **15**, 2060 (2003).